Available online at www.sciencedirect.com
ScienceDirect
Journal of Electroanalytical Chemistry 621 (2008) 322–329
Journal of Electroanalytical Chemistry
www.elsevier.com/locate/jelechem

Porphyrin "Mille-Feuilles" photo-electrodes

Shuxin Tan, Bin Su, Mohamad Hojeij, Hubert H. Girault *

Laboratoire d'Electrochimie Physique et Analytique, Ecole Polytechnique Fédérale de Lausanne, Station 6, CH-1015 Lausanne, Switzerland

Received 22 November 2007; received in revised form 12 February 2008; accepted 13 February 2008
Available online 19 February 2008

Abstract

A porphyrin "Mille-Feuilles" photo-electrode is fabricated layer-by-layer by deposition of anionic [zinc *meso*-tetrakis(*p*-sulfonato phenyl) porphyrin]$^{4-}$ ($ZnTPPS^{4-}$) and positively charged polypeptides on a 11-mercaptoundecanoic acid-modified gold electrode to form a photoactive film. This work demonstrates that it is possible to form 3D structures having regularly spaced layers of redox molecules. UV–visible spectra of the multilayer films display the characteristic absorption bands of the porphyrins and the absorbance increases linearly with the number of bilayers. The cyclic voltammetric response of the films in contact with 1,2-dichloroethane (DCE) varies from that of a modified electrode to that of a supported liquid film. Under illumination, a large photocurrent response for oxygen reduction with a maximum for a 5-bilayer film is observed.

Keywords: Porphyrins; Polypeptides; Multilayers; Layer-by-layer; Photocurrent

1. Introduction

The design of photo-electrodes is a key aspect of solar energy conversion. The main approach relies on semiconductor for the charge separation process. With the goal to mimic photosynthesis, many efforts have been devoted to the development of modified electrodes where a metallic electrode is directly sensitised by a chromophore. Porphyrins in particular have been widely used to produce modified electrodes, either with a monolayer or a multilayer structure. Usually, the dye sensitised metallic electrodes suffer from significant back electron transfer reactions. To circumvent this problem, we have developed the concept of supported interfaces between two immiscible electrolyte solutions (ITIES), where the electrode is covered by a thin aqueous layer and immersed in an organic electrolyte solution. We have shown that it is then possible to sensitise the liquid|liquid interface (ITIES) to vectorise the photo-electron transfer reactions [1–3].

As one of the most suitable and versatile approach to fabricate functional two-dimensional or three-dimensional thin aqueous films, electrostatic layer-by-layer self-assembly based on the work of Decher and co-workers has found many applications in molecular and nanoscience technology [4–7]. The key advantage of this approach is the possibility of assembling a number of different hybrid materials such as polyelectrolytes, biological components, nanoparticles and photoactive dyes [4–10] thanks to the alternate deposition of layers of opposite surface charges. Other important features include the simple deposition process and the possibility to control their organization at the molecular level as well as to control the thickness easily by varying the number of adsorbed layers.

Successful applications of this technique are in the field of photoinduced electron transfer reactions, where the functional two-dimensional or three-dimensional thin films incorporate photosensitisers, which can generate photoelectrons under light illumination [10–12]. It is well known that porphyrins represent an important class of photosensitisers with high extinction coefficients in the visible region. They can be found in chlorophylls as light-harvesting complexes for the natural photosynthetic system

* Corresponding author. Tel.: +41 21 693 3151; fax: +41 21 693 3667.
E-mail address: hubert.girault@epfl.ch (H.H. Girault).

0022-0728/$ - see front matter © 2008 Published by Elsevier B.V.
doi:10.1016/j.jelechem.2008.02.007

[13,14]. The challenge to create artificial mimics of these light-harvesting complexes has stimulated the development of routes to form porphyrin multilayers in polypeptide matrix by electrostatic layer-by-layer self-assembly. Highly conductive metal electrodes are a natural choice for assembling molecular layers with photoelectric functions, and for example thiol-modified gold electrode have been extensively used to assemble a great variety of organic molecules [15].

Recently, we have shown that it was possible to create three dimensional structures by alternate deposition of negatively charges quantum dots (CdSe, CdSe@CdS, ...) and pLys [16], which when immersed in an organic electrolyte solution behave as efficient photo-electrodes for oxygen reduction. In the present study, we demonstrate that alternate multilayers of negatively charged, small and rigid molecules like porphyrins and polycations provide a very efficient route to generate "Mille-Feuilles" structures with photoactive properties, which have been studied at various applied potentials and thicknesses. The goal of this work is to highlight the difference between a modified electrode and a supported ITIES where a second polarised interface is supported on the solid and polarised metal electrode.

2. Experimental

2.1. Chemicals

All chemicals were of analytical grade and used as received unless otherwise described. Poly-L-lysine (pLys, $M_W = 30{,}000$) was purchased from Sigma. Zinc *meso*-tetrakis(*p*-sulfonatophenyl) porphyrin tetrasodium ($Na_4ZnTPPS$) is a product of Porphyrin Products Inc. 11-mercaptoundecanoic acid (MUA), and the solvents (1,2-dichloroethane (DCE) and ethanol) were purchased from Aldrich. Disodium hydrogen phosphate ($Na_2HPO_4 \cdot 2H_2O$), sodium dihydrogen phosphate ($NaH_2PO_4{\cdot}2H_2O$) and bis(triphenylphosphoranylidene) ammonium chloride (BTPPAC1) are Fluka products. Lithium tetrakis(pentafluorophenyl) borate (LiTPFB) was purchased from Boulder Scientific. The organic supporting electrolyte, bis(triphenylphosphoranylidene) ammonium tetrakis(pentafluorophenyl)borate (BTPPATPFB), was prepared as previously reported [17]. The buffer solution with pH 8 was prepared with 0.1 M $Na_2HPO_4 \cdot 2H_2O$ and $NaH_2PO_4 \cdot 2H_2O$. All aqueous solutions were prepared with purified water from a Milli-Q 185 system (18.0 Ω cm).

2.2. Electrostatic multilayer preparation

The gold electrodes were prepared as follows. A 100 nm-thick gold layer was deposited by thermal evaporation on microscope glass slides, which were treated with a Piranha solution and cleaned by sequential sonication in ethanol, acetone and purified water followed by drying under the Argon flow. Before the gold deposition, a 1 nm thick chromium buffer layer was initially deposited on the glass slide to improve adhesion of the gold film. Then, the as-prepared gold electrode was modified with MUA by the formation of gold-thiol bond when the freshly prepared gold electrode was immersed into 1 mM MUA ethanol solution for one night. Loosely bound MUA molecules were removed from the electrode surface by rinsing successively with ethanol and water, and then dried with nitrogen stream. The pLys/$ZnTPPS^{4-}$ multilayers were assembled by the alternatively sequential immersing of the MUA-modified gold electrode into alternating aqueous solutions of 1 g L^{-1} pLys (0.1 M phosphate buffer solution at pH 8.0) and 1 mM $ZnTPPS^{4-}$ solutions, starting with a pLys layer and ending with a $ZnTPPS^4$ layer until the desired number of $(pLys/ZnTPPS^{4-})_n$ bilayers was deposited (Scheme 1). Between each dip, the multilayer film was rinsed with ultrapure water and dried under nitrogen stream. The deposition time for pLys is 20 min, which was assigned by Kelvin probe measurements [18]. The deposition time for $ZnTPPS^{4-}$ was 60 min, as determined by UV–visible absorption spectra. Indeed, no significant increases in absorbance were observed upon immersing the polyelectrolyte layers into aqueous porphyrin solutions for longer times [18]. It is important to stress that $ZnTPPS^{4-}$ are rigid molecules carrying four charges. The principle of layer-by-layer deposition is that the adsorption of each layer provides a surface excess charge, not only compensating the charge of the underlayer. It is crucial that each adsorbed molecule carries more that one charge, behaving as a poly-ion, i.e. an ion for which the solvation energy is the sum of the solvation energies of each ionic moiety. Indeed, it is difficult to do layer-by-layer structure with ions carrying a single charge such as, for example ferrocyanide ($Fe(CN)_6^{4-}$).

2.3. UV–visible absorption and fluorescence measurements

The formation of multilayers of $(pLys/porphyrin)_n$ were monitored by UV–visible absorption spectroscopy (Varian) and luminescence spectrometer (PERKIN–ELMER, LS50B) by depositing directly the multilayers on negatively charged microscope glass slides treated with a Piranha solution.

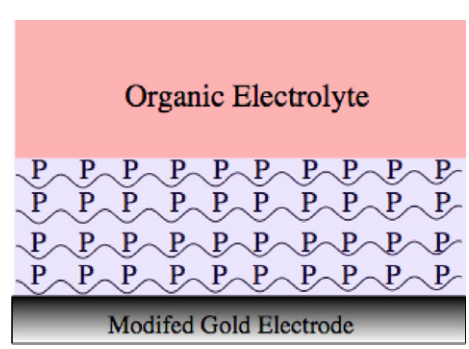

Scheme 1. Representation of the "Mille-Feuilles" photoelectrode.

Scheme 2. The electrochemical cell and electrolyte composition.

2.4. Electrochemical measurements

Cyclic voltammetry of (pLys/porphyrin)$_n$ multilayers in a DCE solution was performed on an Autolab PGSTAT-30 potentiostat (Eco Chemie) in a three-electrode configuration. The corresponding experimental cell and electrolyte composition is illustrated in Scheme 2. The multilayer modified gold slide functions as the working electrode, and a Pt wire as the counter electrode. And the reference electrode was assembled using an Ag|AgCl wire together with a non-polarisable water|DCE interface with $BTTPA^+$ as the potential determining ion. The supporting electrolyte used in DCE is 5 mM BTPPATPFB. All potentials reported refer to the Ag|AgCl electrode.

2.5. Photocurrent measurements

Photocurrent transient measurements of (pLys/porphyrin)$_n$ multilayers were performed in a DCE solution using 5 mM BTPPATPFB as the supporting electrolyte under potentiostatic conditions, where the external potential bias was supplied by a Hi-Tek waveform generator (Hi-Tek Instruments PP-R1). The illumination was carried out with a beam line of 454 nm from an argon ion tunable laser (Omnichrome series 43). An optical shutter with an aperture time in the range of μs was used to control the illumination time. The photon flux was quantitatively determined with a calibrated power meter (Gentec, TPM-310).

3. Results and discussion

3.1. Spectroscopic studies on (pLys/ZnTPPS^{4-})$_n$ multilayers

UV–visible absorption measurements were carried out to monitor the electrostatic layer-by-layer self-assembling process of pLys/$ZnTPPS^{4-}$ multilayer films, and the results are shown in Fig. 1a. It should be mentioned that pLys does not have any appreciable light absorption in the visible region as major transitions occur in the UV region (<300 nm). In the multilayer films, the absorption spectrum of $ZnTPPS^{4-}$ displays a strong Soret band at $\lambda_{max} = 434$ nm and two weak Q-bands at $\lambda_{max} = 563$ nm and 606 nm. These signals suggest a successful film deposition by the electrostatic layer-by-layer approach. Importantly, the absorbance of $ZnTPPS^{4-}$ is increased with the number of depositing cycles, while the shape of the absorption spectra remains stable. By plotting the optical density at 434 nm versus the number of bilayers, a good linear relationship could be obtained, as shown in Fig. 1b. This indicates that the multilayer growth for both pLys and $ZnTPPS^{4-}$ is a stepwise and regular process, resulting in a regular "Mille-Feuilles" structure. From linear fitting, an average increase of the absorbance of 0.045 per bilayer was obtained (correlation coefficient $R = 0.9$).

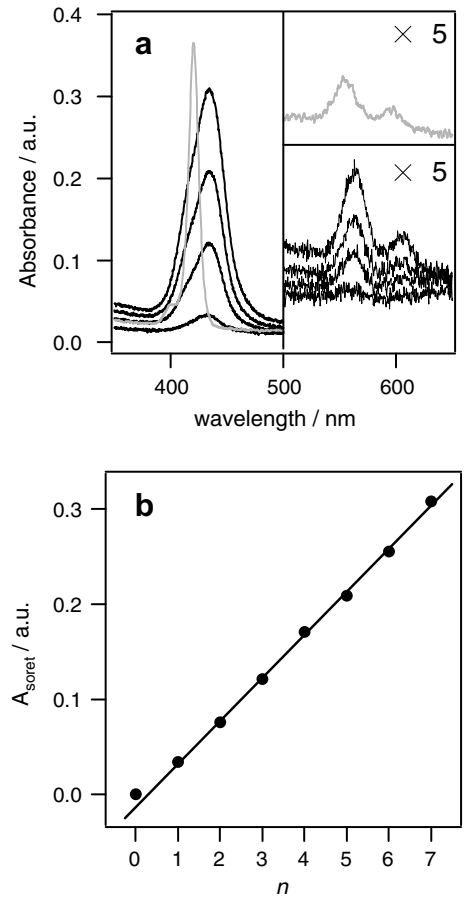

Fig. 1. (a) UV–vis spectra of (pLys/$ZnTPPS^{4-}$)$_n$ multilayers ($n = 1$, 3, 5 and 7) (black lines) and of a $ZnTPPS^{4-}$ dilute solution (gray line). (b) Maximum absorbance at $\lambda_{max} = 434$ as a function of the number of pLys/$ZnTPPS^{4-}$ bilayer.

On the other hand, the Soret absorption band of $ZnTPPS^{4-}$ in the multilayer films solution is broadened and red-shifted in comparison with that of $ZnTPPS^{4-}$ in solution, a narrow Soret band with $\lambda_{max} = 420$ nm. The two weak Q-bands also red-shifted from $\lambda_{max} = 553$ nm and 598 nm to 563 nm and 606 nm. The bathochromic shift in the absorption bands, as well as the broadening of the absorption bands result from the strong electronic interaction between individual porphyrin molecules absorbed in the film. Therefore, Fig. 1 shows that the adsorbed porphyrins are a layer of J-aggregates, which have been observed previously in the layer-by-layer films [19–22].

The emission spectra of (pLys/$ZnTPPS^{4-}$)$_7$ multilayer film excited at a wavelength of 434 nm only show a very weak fluorescence signal (data not shown). In comparison to the two emission bands at 606 nm and 658 nm observed with a $ZnTPPS^{4-}$ dilute solution, the emission spectrum of

multilayer film only displays one weak broad band that shifts to longer wavelengths. This again should corroborate the formation of $ZnTPPS^{4-}$ J-aggregates during the deposition [23].

3.2. Electrochemical behaviour of (pLys/porphyrin)$_n$ multilayers

The electrochemical characteristics of (pLys/porphyrin)$_n$ multilayers was investigated by cyclic voltammetry. Fig. 2 displays CVs of (pLys/porphyrin)$_n$ film ($n = 1$, 3 and 7, respectively) assembled on MUA-modified gold electrode at different scan rates. All the CVs for (pLys/porphyrin)$_n$ film assembled on MUA-modified gold electrode contain one pair of coupled oxidation/reduction current peaks between 0 V and 1.2 V. Whereas, CVs of pLys assembled on MUA-modified gold electrode without porphyrin exhibits only capacitive current within the potential region between 0 V and 1.2 V. Therefore, the observed faradaic current in CVs of (pLys/porphyrin)$_n$ film is attributed to redox reaction of porphyrin unit [$Zn(II)TPPS^{4-}$/$Zn(II)TPPS^{3-}$], which indicates a well-defined electroactivity of the porphyrin in the multilayer structure.

Furthermore, from the CVs of Fig. 2 show that the number of deposited bilayers has a significant effect on the voltammetric response of the multilayer films. For the 1-bilayer film, the anodic and cathodic peak currents increase linearly with the increase of potential scan rate in the range of 0.01–0.1 V s^{-1} (shown in Fig. 3a). This is a voltammetric response of surface bound species for which there is instant charge compensation by ions from the organic phase [24–28]. It is interesting to notice that if the forward peak potential remains constant, the backward peak potential shifts upon increasing scan rates.

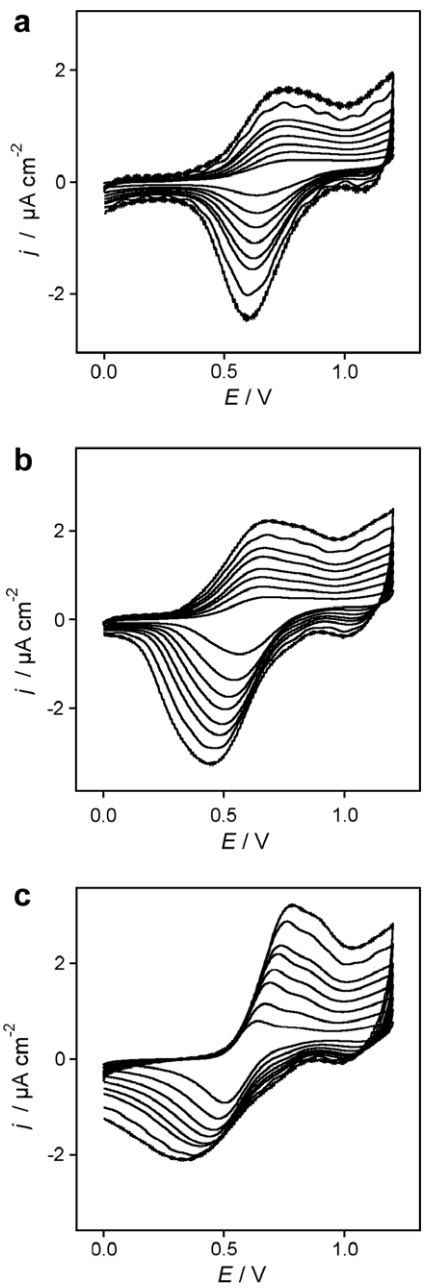

Fig. 2. CVs of (pLys/$ZnTPPS^{4-}$)$_n$ multilayers ($n = 1$ (a), 3 (b) and 7 (c), respectively) placed in contact with DCE containing 5 mM BTPPATPFB at various scan rate: 0.01, 0.02, 0.03, 0.04, 0.05, 0.06, 0.08 and 0.10 V s^{-1} from inner to outer.

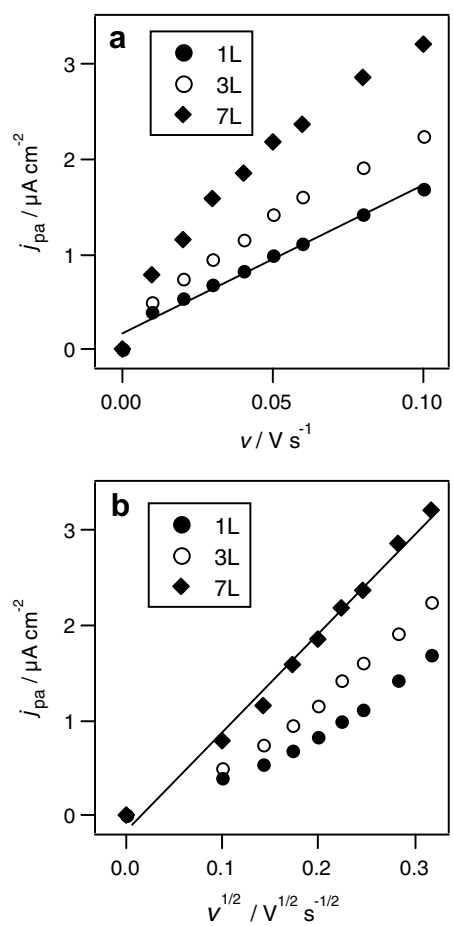

Fig. 3. Dependence of the peak current of (pLys/$ZnTPPS^{4-}$)$_n$ multilayers ($n = 1$, 3, and 7, respectively) on the scan rate (a) and the square root of the scan rate (b).

The forward peak is due to the porphyrin oxidation where an electron transfers from porphyrin molecules/aggregates to the gold electrode across the thiol monolayer and the pLys layer. The forward peak is broad, and such a broadening has been described by White et al to be due to a combined effect of slow kinetics and counter ion mass transport [29]. Collman et al. have also observed such behaviour for porphyrin multilayer modified electrodes and have rationalised the voltammetric response by considering the concentration dependence of the surface activity coefficients [30]. Murtomaki has also recently shown that the observed voltammograms can be analysed in the case of a supported ITIES by considering the potential dependence of the transfer of the counter ion across the liquid|liquid interface. The return peak is narrower but shifts with scan rate indicative in any case of a slow kinetic [31].

As the number of layers is increased, the charge compensation must take place either through ingress or egress ion transfer reactions to maintain the film electroneutrality. On the forward scan, anion ingress or a cation egress, and inversely on the reverse scan, cation ingress or an anion egress are taking place. Considering the species present, the forward scan is likely to be accompanied by a sodium ion egress and the reverse scan by a phosphate or chloride ion egress. All these aqueous ions are incorporated in the film during the layer-by-layer assembly.

As can be observed in Fig. 2, both peaks get broader and further separated as the film thickness increases. For a 7-bilayer film, the scan rate dependence of the oxidation peak current shows a linear relation of the square root of the scan rate as shown in Fig. 3b. This shows that for thick films, mass transport either in the film or to the film plays a role.

From a mechanistic viewpoint, it is most likely that the different layers are oxidized stepwise as observed by the peak broadening. Indeed, the oxidation of the film can be considered as a multi-step process, e.g. for a 5-layer process

$$\mathrm{M{-}(P{-}P{-}P{-}P{-}P)} \xrightarrow{-e^-} \mathrm{M{-}(P^+{-}P{-}P{-}P{-}P)}$$
$$\rightarrow \mathrm{M{-}(P{-}P{-}P{-}P{-}P)^+}$$
$$\mathrm{M{-}(P{-}P{-}P{-}P{-}P)^+} \xrightarrow{-e^-} \mathrm{M{-}(P^+{-}P{-}P{-}P{-}P)^+}$$
$$\rightarrow \mathrm{M{-}(P{-}P{-}P{-}P{-}P)^{2+}}$$

This successive electron transfer reactions to oxidize the film take place at increasing redox potentials, yielding also a peak broadening. The mathematical modeling of this multi-step reaction is beyond the scope of this manuscript, but the "Mille-Feuilles" structure developed is an interesting model of highly layered redox states.

In a previous communication, we endeavoured to distinguish a modified electrode from a supported interface between two immiscible electrolyte solutions (ITIES). In the former, the potential drop between the metallic electrode and the organic solution spans across the film. In the latter, we have two distinct polarised interfaces in series, the centre of the film being electroneutral. The potential difference between the electrode and the organic electrolyte solution is then distributed first at the metal–film interface and then at the film–organic electrolyte solution interface. In this case, this interface is a classical polarised liquid–liquid interface called ITIES. When the film is made of bilayers of pLys and pGlu (poly-glutamate) we had shown that the transition between a modified electrode and a supported ITIES occurs when the film thickness is 5-bilayers thick.

The voltammograms in Fig. 2 also show that the current is proportional to the number of porphyrin layers showing all the layers are oxidized as illustrated in Fig. 4 in the case of the peak current at different scan rates.

3.3. Photoinduced charge transfer properties

Fig. 5 shows photocurrent transients of porphyrin multilayers of different thicknesses at negative applied potentials. There is no faradaic response in this potential range prior to illumination, and upon illumination fast cathodic photocurrent responses can be observed associated to the photoreduction of oxygen in the film. Generally, the initial photocurrent of a photosensitive film coated electrode is only associated with the photo-oxidation and photoreduction of the film and it can be simply expressed by [3,32]:

$$j^0_{\mathrm{ph}} = \Phi\left(k^*_{\mathrm{ox}} - k^*_{\mathrm{red}}\right) \tag{1}$$

where k^*_{ox} and k^*_{red} are the respective electron transfer rate constants (s^{-1}) from the excited film to the gold surface (photo-oxidation) or from the gold electrode to the excited film (photoreduction) as illustrated in Scheme 3. The parameter Φ is defined by:

$$\Phi = \frac{FAI_0}{N_A k_r} \tag{2}$$

where F, A, I_0 and N_A denote Faraday's constant, the absorbance of the film, the incident light intensity and Avogadro's constant, respectively. k_r is the average rate constant assigned to the decay of the excited state of the

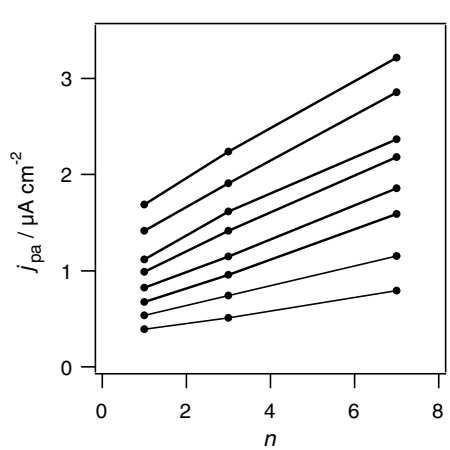

Fig. 4. Dependence of the peak current of $(\mathrm{pLys/ZnTPPS^{4-}})_n$ multilayers on the number of layers for different scan rates.

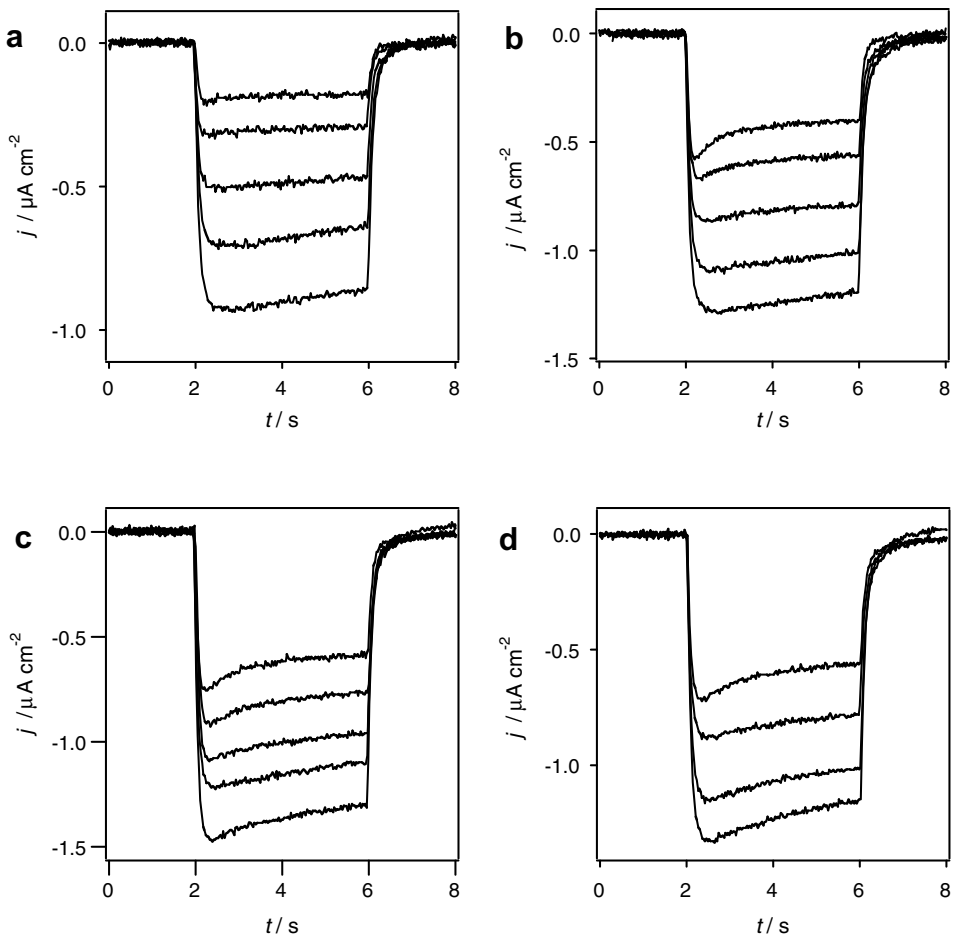

Fig. 5. Photocurrent transients of (pLys/ZnTPPS^{4-})$_n$ multilayers ($n = 1$ (a), 3 (b), 5 (c) and 7 (d), respectively) at various applied potentials: −0.4, −0.3, −0.2, −0.1 and 0 V from bottom to top.

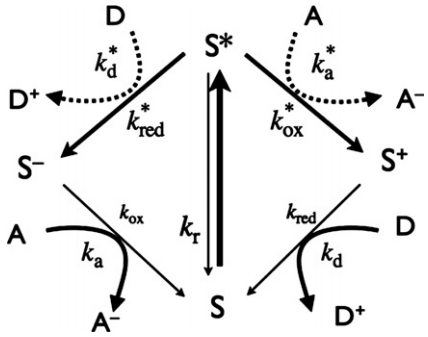

Scheme 3. Model of the photoinduced electron transfer reactions. (S) represents the porphyrin sensitizer and (D) is an electron donor and (A) is an electron acceptor.

porphyrins. Here, the porphyrin lifetime is in the order of microseconds. When only a photocathodic current is observed, the photoreduction is dominant and we have $k^*_{red} \gg k^*_{ox}$. In this case, Eq. (1) reduces to:

$$j^0_{ph} = -\Phi k^*_{red} = -\frac{FI_0 k^*_{red}}{N_A k_r} A \quad (3)$$

Then, due to the recombination reaction, the photocurrent decays slowly with time. As can be observed from Fig. 5, the thicker the film the stronger the decay. For thin films, the photocurrent is pseudo steady-state and the rate limiting step is the electrode reaction. For thick films, the chemical re-oxidation of the reduced porphyrins by oxygen is not fast enough to maintain a steady-state photocurrent. The film being an aqueous one, it is possible that the re-oxidation reaction by molecular oxygen takes place at the film/organic solvent interface as the solubility of oxygen is higher in the organic phase. When the irradiation is off, the photocurrent decreases quickly to zero, and no recombination overshoot can be observed. It should be mentioned that no photocurrent is observed in the absence of porphyrins in the film.

From Eq. (3), we can obtain the potential dependence of the electrochemical reduction rate constant k^*_{red}. As illustrated in Fig. 6, it is interesting to notice that for thin films, the rate constant increases whereas, for thicker films it decreases. This observation confirms previous studies showing that for less than five bilayers a modified electrode behaviour is expected where the overall potential difference between the metal and the organic phase is spread across the film, and resulting here in different potential dependent kinetics. For film thicknesses larger than five bilayers, a

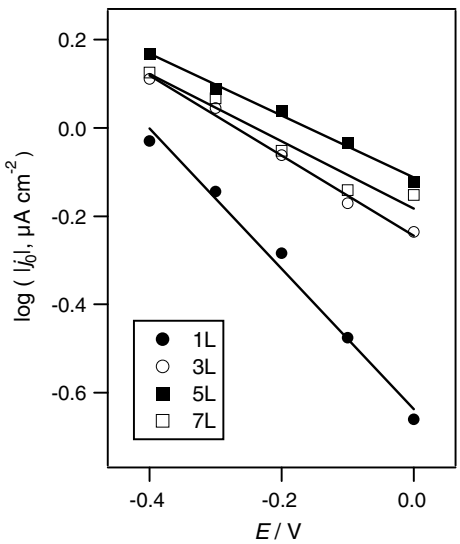

Fig. 6. The initial photocurrent as a function of the applied potential for various thickness of the films.

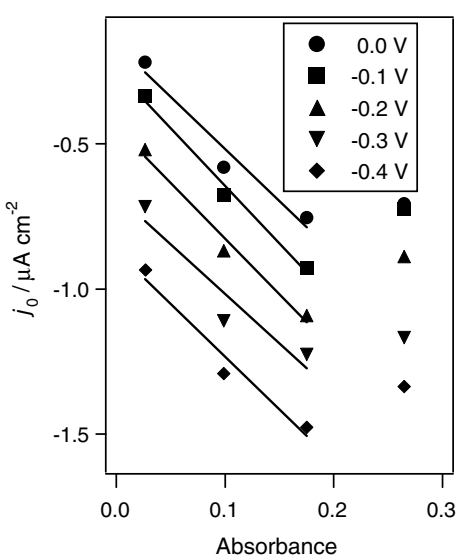

Fig. 7. The initial photocurrent as a function of the film absorbance for various applied potentials.

supported thin liquid film behaviour is expected, where the overall potential difference occurs at the metal–film interface and at the film/organic phase interface. As a result here, the rate constant k^*_{red} is maximum for a 5-bilayer film.

This distinction between modified electrode and supported film behaviour can also be observed when comparing the initial photocurrent as a function of the absorbance as illustrated in Fig. 7. We can see that the photocurrent magnitude at different applied potentials increases up to five bilayers, and then decreases.

4. Conclusion

Porphyrin multilayer films were assembled with polypeptides on MUA-modified gold electrodes using a layer-by-layer approach. The resulting "Mille-Feuilles" structure is confirmed by UV–visible absorption spectra. The porphyrins deposited form J-aggregates on the top of each polypeptide layers. The electrochemical response of this "Mille-Feuilles" modified electrode was studied in an organic electrolyte solution immiscible with water, so as to trap of the water-soluble species within the aqueous layer. Cyclic voltammograms and photocurrent measurements were performed to characterize charge transfer processes under dark and illumination conditions. It is shown clearly that thin pLys/ZnTPPS^{4-} films behave as modified electrodes, whereas thicker films behave as supported aqueous films. The photocurrent response clearly shows that the present approach can be developed to design photo-electrodes with a large photo capture cross-section and efficient vectorisation.

Acknowledgements

This work is supported by the Swiss National Science Foundation (200020-105486) and Ecole Polytechnique Fédérale de Lausanne (EPFL).

References

[1] J.J. Kakkassery, D.J. Fermin, H.H. Girault, Chem. Commun. (2002) 1240.
[2] S. Tan, M. Hojeij, B. Su, G. Meriguet, N. Eugster, H.H. Girault, J. Electroanal. Chem. 604 (2007) 65.
[3] M. Hojeij, N. Eugster, B. Su, H.H. Girault, Langmuir 22 (2006) 10652.
[4] G. Decher, J.D. Hong, Makromol. Chem. 46 (1991) 321.
[5] G. Decher, Science 277 (1997) 1232.
[6] G. Decher, B. Lehr, K. Lowack, Y. Lvov, J. Schmitt, Biosens. Bioelectron. 9 (1994) 677.
[7] G. Schneider, G. Decher, N. Nerambourg, R. Praho, M.H.V. Werts, M. Blanchard-Desce, Nano Lett. 6 (2006) 530.
[8] J.-W. Choi, Y.-S. Nam, J.-M. Kim, J.S. Kim, J. Nanosci. Nanotechnol. 6 (2006) 3526.
[9] Z. Liang, K.L. Dzienis, J. Xu, Q. Wang, Adv. Func. Mater. 16 (2006) 542.
[10] K.Y.K. Man, C.W. Tse, K.W. Cheng, A.B. Djurisic, W.K. Chan, J. Inorg. Organomet. Polym. Mater. 17 (2007) 223.
[11] L. Sheeney-Haj-Ichia, S. Pogorelova, Y. Gofer, I. Willner, Adv. Func. Mater. 14 (2004) 416.
[12] D.M. Guldi, F. Pellarini, M. Prato, C. Granito, L. Troisi, Nano Lett. 2 (2002) 965.
[13] Q. Wang, W.M. Campbell, E.E. Bonfantani, K.W. Jolley, D.L. Officer, P.J. Walsh, K. Gordon, R. Humphry-Baker, M.K. Nazeeruddin, M. Graetzel, J. Phys. Chem. B 109 (2005) 15397.
[14] M. Schellenberg, P. Matile, J. Plant Physiol. 146 (1995) 604.
[15] M.D. Porter, T.B. Bright, D.L. Allara, C.E.D. Chidsey, J. Am. Chem. Soc. 109 (1987) 3559.
[16] M. Hojeij, B. Su, S. Tan, G. Meriguet, H.H. Girault, submitted for publication.
[17] B. Su, J.-P. Abid, D.J. Fermin, H.H. Girault, H. Hoffmannova, P. Krtil, Z. Samec, J. Am. Chem. Soc. 126 (2004) 915.
[18] J.J. Kakkassery, Ph.D Thesis, Ecole Polytechnique Fédérale de Lausanne, Lausanne, 2004.
[19] Y. Sun, X. Zhang, C. Sun, Z. Wang, J. Shen, D. Wang, T. Li, Chem. Commun. (1996) 2379.
[20] K. Ariga, Y. Lvov, T. Kunitake, J. Am. Chem. Soc. 119 (1997) 2224.

[21] P.G. Van Patten, A.P. Shreve, R.J. Donohoe, J. Phys. Chem. B 104 (2000) 5986.
[22] Y. Egawa, R. Hayashida, J.-I. Anzai, Langmuir 23 (2007) 13146.
[23] N.C. Maiti, S. Mazumdar, N. Periasamy, J. Porphy. Phthal. 2 (1998) 369.
[24] F.M. Raymo, R.J. Alvarado, E.J. Pacsial, D. Alexander, J. Phys. Chem. B 108 (2004) 8622.
[25] D. Laurent, J.B. Schlenoff, Langmuir 13 (1997) 1552.
[26] H. Zheng, Y. Hirose, T. Kimura, S.-I. Suye, T. Hori, H. Katayama, J.-I. Arai, R. Kawakami, T. Ohshima, Sci. Technol. Adv. Mater. 7 (2006) 243.
[27] A. Liu, Y. Kashiwagi, J.-I. Anzai, Electroanalysis 15 (2003) 1139.
[28] A. Narvaez, G. Suarez, I.C. Popescu, I. Katakis, E. Dominguez, Biosens. Bioelectron. 15 (2000) 43.
[29] C.P. Smith, H.S. White, Anal. Chem. 64 (1992) 2398.
[30] I.M. Shiryaeva, J.P. Collman, R. Boulatov, C.J. Sunderland, Anal. Chem. 75 (2003) 494.
[31] L. Murtomaki, 2007, private communication.
[32] S. Tan, B. Su, C. Roussel, H.H. Girault, Inorg. Chim. Acta 361 (2008) 746.